

Influence of Geometrical Shape on the Crashworthiness Performance of Tubular Jute Mat/Epoxy Composite Specimens

Sabah Salim Hamza^{1,2,*}, AL Emran Bin Ismail¹, Mohd. Yuhazri Yaakob³, Salih Meri AL Absi⁴.

¹Faculty of Mechanical and Manufacturing Engineering, University Tun Hussein Onn Malaysia (UTHM),

² Al muthana Water Directorate, General Directorate of Water, Ministry of Municipalities and Public Works, Iraq

³ Faculty of Mechanical and Manufacturing Engineering Technology, Universiti Teknikal Malaysia Melaka Hang Tuah Jaya, 76100

⁴Iraqi Cement State Company, Ministry of Industry and Minerals, Baghdad, Iraq

* Corresponding author: hd160005@siswa.uthm.edu.my

Abstract-- Nowadays, the interest in using natural fibers reinforced plastic have been increased dramatically in many engineering applications due to its distinctive properties such as low density, good Energy-absorbing capacity, and is considered environmentally friendly. In the present paper investigated experimentally the crashworthiness characteristics and corresponding energy-absorbing capability of different geometrical shapes under quasi-static loading of natural tubular jute mat/epoxy composite structures. The purpose is to determine the appropriate design of natural compounds, which can provide the potential to substitute conventional structures currently in use. Two different geometrical shapes (corrugated and circular tubes) were fabricated by a combination manual lay-up and vacuum-bagging moulding techniques, specimen thickness (2, 3 and 4 laminate plies), tulip triggering and 100mm in length, and then the post-curing has been conducted on graded temperature treatment. The influence of cross-section shape, number of laminate plies, and temperature treatment on crashworthiness characteristics under quasi-static loading were examined and discussed. From this unique study, Laboratory results indicate that most of the specimens failed in a stable and progressive manner. However, the corrugated cross-sectional shapes with three layers are considered optimum design in terms of energy-absorbing, peak load, average load, and crushing efficiency for crashworthiness tubes application.

Index Term— Natural fibres, geometrical shapes, quasi-static, crashworthiness, energy absorption, peak load

1. INTRODUCTION

Recently, interest in environmental problems has been increased among researchers; the natural fibers are gaining considerable attention by authors and manufacturers in the direction of replacement of synthetic composite fibers especially in the automotive industry field due to their characteristics such as lower weight, good in strength and elastic modulus, biodegradable, renewable, recyclable, eco-friendly, available abundantly, and low cost [1-2]. Fundamentally, weight is a key criterion as well as to crashworthiness in the motor vehicle Engineering field. The minimum weight corresponds with a decrease in fuel consumption and carbon dioxide emissions, thus it contributes to the protection of the environment [3-4].

Nowadays, the usage of transportation, especially automotive have become an important part of daily life. However, the rapid development of the vehicle industry and increasing their numbers, so that drive to more traffic accidents, that lead to death or serious injuries. Therefore, the safety factor is a very important issue [5]. The major function

of the crashworthiness is absorption of the impact energy, protecting the occupant's compartments and to ensure the maximum force transmitted to occupants is lower in case a collision event [6]. Several investigates have been conducted on crashworthiness performance by using metals [7], and synthetic composite materials [8], whilst few of the number of studies by using the natural composite fibers [9]. according to previous researches, to understand absorption of the impact energy, a few parameters such as type of material, cross-section shapes, and specimen geometry(layers numbers, length, and diameter to thickness ratio) [10-11] in addition to the temperature treatment [12] and so on. That influence the crashworthiness of structure (e.g.: maximum peak load (Pmax), mean load (Pm), energy absorption (EA), and crushing efficiency η_c) are chosen.

As a part of industrial applications, large interest is given to fabricate natural composite structures and testing them to replace metallic and synthetic composite products. The authors employ these studies in axial crushing behaviours and total energy dissipation [13,14]. An enormous of published papers have used quasi-static compression to investigate the crashworthiness characteristics of composite and metal specimens [15-18]. The merit of this approach is that the testing procedures take place at a slow speed, thereby it provides a means to control the crushing process and capture pictures for each phase of the test sample. Thus, it can present a better choice to reject the composite specimen which shows catastrophic or non-progressive failure modes.

There is a consensus among researchers that geometry of specimen is an important variable in influencing the level of energy absorption. Palanivelu et al.[19] Reported that the geometric shapes and dimensions of composite material structures are two variables that play a very important role in influencing absorption energy device. Abdewi et al.[20] Investigated the effectiveness of tube geometry on the energy absorption (EA) of tubular composite structures. He concluded that by an alter in cross-section that leads to a growth in modulus which in turn a rise in deformation strengths and energy dissipate. Ross et al.[21] studied theoretically and experimentally the buckling pressure of hemi-ellipsoidal domes which made from GRFP. Three aspect ratio of oblate domes were tested under external pressure. It concluded that, when the ratio of dome height/base radius increased from 0.25 to 0.7, the produced buckling pressure

increased by (0.420 to 0.900). McGregor [22] reported that the highest energy absorption capacity when using circular section specimens compared to square and rectangle cross-section specimens. Rabiee et al. [23] stated the "I" cross-section tubes. Based on the experimental work, it demonstrated that the square cross-section of the composite tubes has the ability to absorb energy by 15% more than the composite tube with the "I" cross-section configuration. Azimi et al. [24] investigated experimentally the effect of the cone frusta tubes on energy absorption capability. The study concluded that the energy absorption capacity is positively proportional to the decrease in semi-apical angles of tubes. Abdewi et al.[5] studied the comparison between the shapes of the corrugated cross-section and the circular configuration composite tubes of crushing performance. The study concluded that the corrugated section shape is more effective for energy absorption and crushing efficiency. Briefly, based on the above literature studied, the shapes of the circular and corrugate cross-section tubes produces outstanding behaviour compared to the other geometric shapes tested.

Other studies have been addressed the effect of dimensions on composite tubes, Rezaei et al. [25] studied the effect of the size of the inner diameter and the number of layers on the cylindrical E-glass/epoxy composite tubes with the same other parameters. It concluded that the energy absorption capacity increases up to 31.20% with the increase of the inner diameter size for the cylindrical specimen from 40 to 50 mm, as well as when an increase laminate plies up to double times results increment of steady crushing force up to three-time and SE up to 1.39 times. Yan et al. [4] studied the influence of internal diameter, length/diameter ratios and layers number of flax fibers/epoxy circular specimens on the crashworthiness parameters. The energy absorption capability is strongly influenced by the geometry of the tube. The number of laminated layers with a considerable length of specimen contributes to the higher energy dissipated capability. Moreover Ismail et al.[2] searched the crashworthiness characteristic of tubular natural kenaf fibres/epoxy composite specimens. The study pointed out to the possibility of obtaining higher energy absorption (EA) when using increase layers numbers from two to three plies (increase thickness from 5-7 mm).

On other hand, some studies have examined the effect of temperature treatment on crashworthiness characteristics. Xu et al. [26] studied the effect of temperature treatment on the crashworthiness characteristics of different carbon fibers hybrid specimens by using Aramid, Carbon, and Glass fibers under quasi-static loading. It concluded that carbon/aramid of (A/C2.2, A/C1.6, and A/C2) increase energy absorption capability by 19.2%, 18.4%, and 11.7% respectively through temperature treatment in 100 °C for 200 h. However, there was no obvious difference in results for GF/CF and CF/CF specimens comparing to the specimens that have not undergone temperature treatment. Moreover, these result similar to the previous study by Y. Ma et al. [27].

Large Previous studies [28-30] have demonstrated the fibers orientation along with the axial direction of the tube structure is capable to absorb more energy than other fiber orientations. Therefore, the uni-directional fibre configuration

with the above-mentioned factors has been chosen for this work.

In order to avoid catastrophic failure of composite materials due to the transmit loads to the whole profile structure, thus, the trigger mechanism contributes significantly to obtain gradual failure by concentrating the loads on the edge of the profile structure [31]. Reported by Sivagurunathan et al [32], the tulip triggering mechanism can be considered as a favourable design compared to other trigger mechanisms. Therefore, depending on the above-mentioned facts, TT configuration mechanism would be more applicable in the current study.

Based on previous research, the geometric shapes of the corrugated and circular cross-section specimens are the most effective structures in crashworthiness characteristics. However, it was no study found on the effect of the corrugated cross-section form of natural composite materials on energy absorption capacity yet. Furthermore, the typical characteristics of Natural jute fiber such as low density, reasonable tensile strength, good elastic modulus, readily available and excellent performance relative to the cost-effective [33]. Rarely works have been carried out to study the crashworthiness characteristics by using jute fibers as we seen in the previous literature review. That was the main motivation behind this study. Hence, this search will help to provide more information to the prior contributions to crashworthiness knowledge. Circular composite specimen (CCS) was manufactured and tested in the same conditions to evaluate the result of energy absorption parameters between both two geometric shapes. The effects of layers numbers on the crashworthiness characteristics of composite structures, different layers numbers and comparing results between improved specimens by temperature treatment and specimens without temperature treatment have been considered in current work. In order to evaluate the structure, the parameters such as the (EA, SE, Pmax, pm, η_c , and the failure crushing mechanism) were presented. Two different structures of natural composite have been fabricated by the principle of a combination of simple manual lay-up and vacuum bladder technique method using jute fibers and epoxy resin. All details in following section.

2. EXPERIMENTAL PROGRAM

I. Specimens' Geometry and Materials

Two kinds of tubes have been studied, Composite tubes with corrugated (RCS) and circular (CCS) cross-section form. both types of tubes were fabricated of jute mat form of 1.3 gm/cm³ as reinforcement and Epoxy resin Auto-Fix (1710-A) and Hardener Auto-Fix (1345-B) as a matrix. All tubes made in the same conditions with different number of plies equal to (two, three, and four) with bi-directional orientation fibers. All details of dimensions for tubes' geometry are list in Table 1.

Table I
Details of dimensions of jute/epoxy composite specimens.

Type of specimen	Number of layers	Height, h (mm)	Mean diameter, dm (mm)	Upper diameter, do (mm)	Circle diameter, d (mm)
RCS	2, 3, 4	100	38	50	
CCS	2, 3, 4	100	-	-	50

II. MANDRELS PREPARATION

The second step in the procedure is the preparation of a hollow mandrel. Three geometrical shapes of mandrels were used (corrugated and circular cross-section). All mandrels were made by CNC at the workshop from aluminium alloy with 100 mm height, 50 mm outside diameter, curvatures radius of 6 mm around the sharp angles were machined to reduce the stress on profile corners. As depicted in Fig. 1 the mandrels are then wrapped with plastic to prevent the specimens from sticking to the mould, with this process could facilitate the extraction of the specimens from the mould.

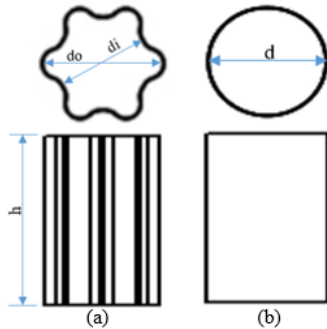


Fig. 1. Sketch diagram for (a) corrugated, and (b) circular cross-section of specimens

III. COMPOSITE FABRICATION

The principle of a combination of manual lay-up and vacuum bladder technique was employed. For facilitating to the removal of the specimen from the mould, wipe the releasing agent on the surface of the mandrel was applied. The jute mat was trimmed to the proper size of the mould, and then weighed for equivalent epoxy use of the layers. Epoxy and hardener were mixed by an electric mixer at ratio (1:1) as per the supplier's instructions. The electric mixer was used in order to prevent air bubble formation in a mixture. The epoxy resin was poured and spread by using a brush onto the jute layers and then wrapping of the fiber around the mandrel. A steel roller was moved over each jute-epoxy layer under a mild press down to dispose of air bubbles from the laminate and to obtain the required thickness. The peel/release ply, release film, and bleeder film were cut as per the mould size and placed on the surface of layers. The whole specimen was sealed by using a vacuum bag under constant vacuum pressure of 6 bars. Under vacuum, Air bubbles were eliminated and distribution the resin into composite laminate equally. The fabricated specimens were left to cure for 24 h at room temperature ($27^{\circ}\pm 2\%$). After that, the specimens were extracted from the vacuum bagging and mould. The post-curing was carried out by placing samples into a heat oven at 60° for 8h and 100° for 4 h. Finally, all tubes were cut into the required specimen size with a height of (100 mm) by using bench saw; a tulip trigger was done by using an angle grinder for each one. This process was repeated four times for each specimen.

IV. EXPERIMENTAL TESTING PROCEDURE

All the tests were done under the same conditions for all tubular specimens. Testing of the specimens was performed by applying uniaxial quasi-static compression forces using an Autograph AG-X. In addition, Shimadzu Universal Testing Machine with a 100 kN loading capacity was used, UTEM, Melaka, Malaysia. The testing was conducted based on ASTM: D7336M-16 with stroke set to 80 mm. The crosshead speed

was at rate 10 mm/min. Each specimen was positioned on the lower fixed platen and were crushed axially by the parallel platen. Four replicate tests were done for each type of sample with different layers number. Crashworthiness characteristics for each sample can be found from the load-deformation graph under compressive force as depicted in Fig. 2.

- Peak load (P_{max}): it is maximum deformation load at the first and second regions with the neglect of the compaction region.
- Mean deformation load (P_m): it is the result of dividing the total energy absorption (EA) in the post-deformation region to the post-displacement displacement (δ), where, $P_m = \frac{AE}{\delta}$ (J/mm).
- Absorbed deformation energy (AE): it represents the work done of the deformation process, it is calculated as the area underneath the curve of a load-deformation response.
- Specific energy dissipates (SE): it is the ratio of work (AE) done to the crushed mass (m) of the specimen, where, $SE = \frac{AE}{m}$ (J/g).
- Deformation load efficiency (η_c): it is calculated from the equation the division of the average load over the greatest deformation load, higher ratio when to be close to unity, where, $\eta_c = \frac{P_m}{P_{max}}$

3. RESULTS AND DISCUSSION

The typical force-displacement graph can be distributed into three outstanding regions as in Fig.2. The first region I represents pre-crushing phase, in which the load (P) increases dramatically and reaches an initial maximum load P_{max} within elastic failure behaviour before dropping. In the second region (II), the load fluctuated about a mean load over the crushing process in the plastic failure region and its associated the post-crushing phase. The force-displacement graph exhibited the P_{max} , P_m and the displacement of the final failure. In the third region (III), known as the compaction phase, the load increases drastically and non-linearly because of debris accumulations at the end of the tube. This region was not taken into account due to its small absorb energy compare with post-crushing region. The test result was detailed in the next section.

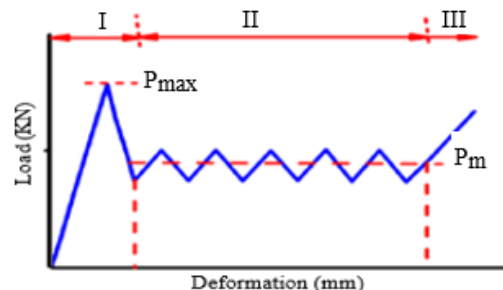


Fig. 2. typical load-deformation graph

- 3.1 LOAD (KN) VS DISPLACEMENT (mm) RESPONSE AND COLLAPSING HISTORY
- 3.1.1 Circular cross-sectional specimens (CCS)

For 2 layers. The load versus axial deformation history for circular JFRP composite tube with two layers is shown in Fig. 3. Obviously in initial phase, the load increase non-linearly until reached 4.809 kN at 19.948 mm displacement as shown in the bottom of Fig. 3, which represents the initial peak load. Then, slightly drops at the pre-crushing zone before it starts to fluctuate around the mean load, which indicates to combination of the lamina bending failure and brittle fracture mode. Lamina bundles experience some bending and fracture close to the end of the tube because of the movement of the upper platen. In the post-crushing phase, the maximum load was 5.284 kN at 36.353 mm displacement, referring to the resistance of the tube to the test load. When displacement reached 58.433 mm, the load decline to minimum value was observed. This phenomenon was due to the local bulking occurred in mid of rest of specimen. This was attributed to the effect of geometry on the failure behaviour of the structure as reported by Luo et al. [34] and Mahdi et al. [35]. At compaction zone, when the crushing reaches at 80 mm displacement, the load dramatically escalated due to the accumulation and the Intensification of crushed composite materials. As a result, the tube contributed the majority of energy absorption through brittle crushing failure (mode II and mode III). Lamina bundle bending, transverse cracks, number of axial cracks, fracture of fibers bundles and matrix were presented along the specimen.

For 3 layers. Fig.4 shows load-displacement diagram and crushing history for circular JFRP specimen with three layers. In the pre-crushing phase, the load increase non-linearly up to reached 12.130 kN at 19.948 mm displacement occurred. And then after slight displacement, uniform fluctuate loads are established around the mean load. This was indicate to the lamina bending failure accompanied by brittle fracture mode from top of tube at the post-crushing phase. In addition, various reasons such as micro-cracks, intra and interlaminar delamination, fibres bridging, mixed-mode fractures were observed along the specimen. As a result, the tube contributed a substantial amount of crushing energy absorption (Mode I and mode II) with shows steady and progressive deformation during the test. This result is in the line with the reported by Hadavinia et al. [36]. When the load reached the value of 5 kN, the compaction phase started. The load escalated rapidly indicating to debris accumulate and crushed material densification. The mainly of energy absorption was through lamina bending, brittle fracture, fragmentation, continuous fibers delamination, axial cracks, and the contribution of friction.

For 4 layers. Fig.5 illustrates the load vs displacement and deformation history for circular JFRP specimen with four layers. In the pre-crushing phase, it can noticed the load increased non-linearly up to reached the first peak load of 10.483 kN at 24.641 mm displacement. At this phase, the load slightly dropped and then after slight displacement, the curve rose and began to fluctuate around the mean load. This was indicated to Progressive deformation manner with diamond buckling mode in a two-sided, and companied with splaying other two side in post-crushing phase. The specimen exhibited brittle and ductile failure manner similar with result by Roslan et al. [37]. At this region, the maximum load value was 14.063 kN at 58.564 mm displacement. Axial cracks along the tensioned lamina bundles among folded layers, lamina bundles bent outward and inward in two side of specimen ,

and local delamination occurred during diamond buckling without fracture as shown at the top of the Fig. 5. Consequence, the tube contributed a significant energy absorption (mode II+III). This phenomenon was due to the increase in the number of layers and its effect on failure behaviour of specimen, which is similar as reported by Belingardi et al. [38]. When the load reached a value of 5kN in the compaction phase, the load escalated rapidly due to crushed material accumulates. The main absorb energy was fragmentation at the onset of crushing, followed by combination a lamina bundles bent and diamond failure buckling.

3.1.2 Corrugated cross-sectional specimens (RCS)

For 2 layers. Fig.6 illustrates the load versus displacement diagram and crushing behaviour history for corrugated JFRP specimen with two layers. Initially, at the pre-crushing zone, the load increased non-linearly up to reach the first peak load of 4.881 kN at 22.661 mm displacement and then slightly drop before it started to oscillate around the mean load, which is indicates to splaying failure manner in the post-deformation phase. Long axial cracks, which developed through the matrix and between layers while leaving most of the fibers bundles intact. As the crush zone progresses down the structure the laminae bent and split into smaller sections of fronds, and a large central wall crack is produced. At the post-deformation zone, the maximum peak load was 6.176 kN at 61.685 mm displacement. As a result, the tube contributed a substantial amount of crushing energy absorption (Mode I) with shows steady and progressive deformation throughout the test. The geometry of the specimen helped to concentrate stress in the curvature of the tube from the top and along its length. Similar conclusion by Abdewi et al. [5] and Eyvazian et al.[39]. They reported that this phenomenon was because of the effect of the geometrical shape of the corrugated tube on failure manner of composite structures. After the curve reached at 83 mm of displacement, the load began with increase drastically due to crushed material accumulates in compaction phase. The most mainly energy absorption was through frictional between the fronds and debris wedge and from another hand between the surface and platen, longitudinal cracks growth, fractures surface, with fibre delamination.

For 3 layers. The load versus displacement diagram and deformation trace for corrugated JFRP specimen with three layers is shown in Fig.7. In the pre-crushing phase, the load escalated non-linearly up to attains initial peak load of 13.101 kN at 20.277 mm displacement and then started to fluctuate and progressively around mean load with the stable manner during post-crushing phase. The longitudinal cracks were noted only at the curvature locations from the top and along its length due to the stress concentration at the curvature of the corrugated surface composite pattern. A splaying manner is characterized by very long cracks. The lamina bundles were not fractured as it underwent bending deformation. At this post-crushing phase, the maximum peak load was 14.399 kN at 59.323 mm displacement. This was for owing to hoop constraint resulting from the axial crack opening along its length of the specimen wall due to the concentration of stress at the curvature of the corrugated composite specimen. In addition, geometry plays a serious role in the influence on the failure mechanism. As a result, the tube contributed a substantial amount of crushing energy absorption (Mode I) with shows steady and progressive deformation throughout

the test. When the load exceeded 80 mm displacement, it began to increase dramatically due to crushed materials accumulated during axial loading apply as it reached compaction phase. The principal energy absorption was through cracks developed along the axial specimen wall, bending of lamina bundles, and contribution of friction effect between the steel platen surface, fronds, adjacent lamina, debris wedge, as well as delamination. This phenomenon in same line with stated by Rabiee et al [23] and Lau et al. [40].

For 4 layers. The load versus displacement diagram and deformation trace for a corrugated JFRP specimen with four layers is an illustration in Fig.8. In the pre-crushing zone, the load grew up non-linearly until it reached the first peak load of 16.252 kN at 28.864 mm displacement and then slightly dropped before it started to oscillate around the mean load, which is referring for the splaying failure manner in the post-deformation phase. Large amounts of the circumferential delamination in the middle thickness of the specimen occurred was noticed during the starting post- crushing phase until the end. In addition axial cracks, micro fracture, and lamina

bundle bending along its length. This phenomenon may be attributed to the uniform corrugated profile that had assisted a formation of axial cracks by stress concentration on the cross-section curvature and hence lamina bundles were formed. The similarity in this conclusion with reported by Alkbir et al. [1], and Palanivelu et al. [41]. The load resistance grew up promptly to reach a maximum peak value of 17.214 kN at around 39.99 mm before the reduction of the load again. This occurred due to the presence of compressed fronds under the movement of the platen downward towards the end of the post-crushing phase. Consequently, the specimen contributed a substantial amount of crushing energy absorption (Mode II and III). After the load reached to 9.445 kN in the compaction phase, the load escalated dramatically that indicated to crush materials accumulate and mass densification. The essential amount of energy was by incorporation of splitting, delamination, bending, multi micro-cracks including fibers fracture and matrix, and friction.

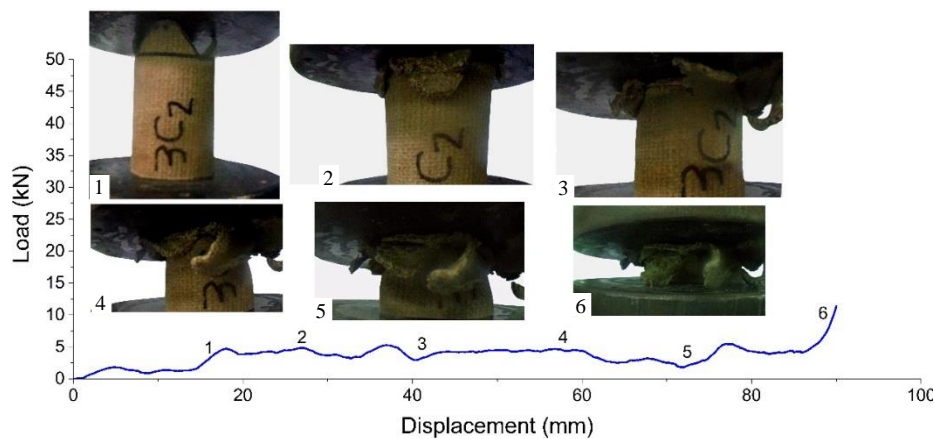


Fig.3. Representative Load vs displacement and collapse history of Circular with 2 layers specimen

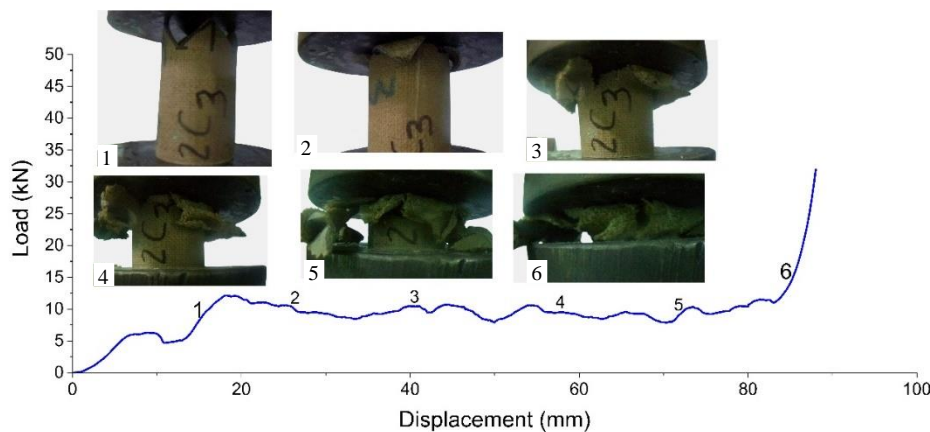


Fig.4. Representative Load vs displacement and collapse history of Circular with 3 layers specimen

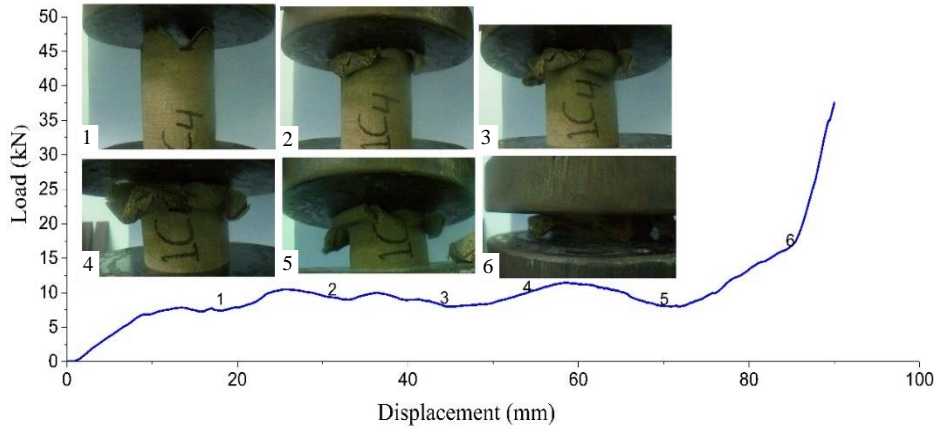


Fig.5. Representative Load vs displacement and collapse history of Circular with 4 layers specimen

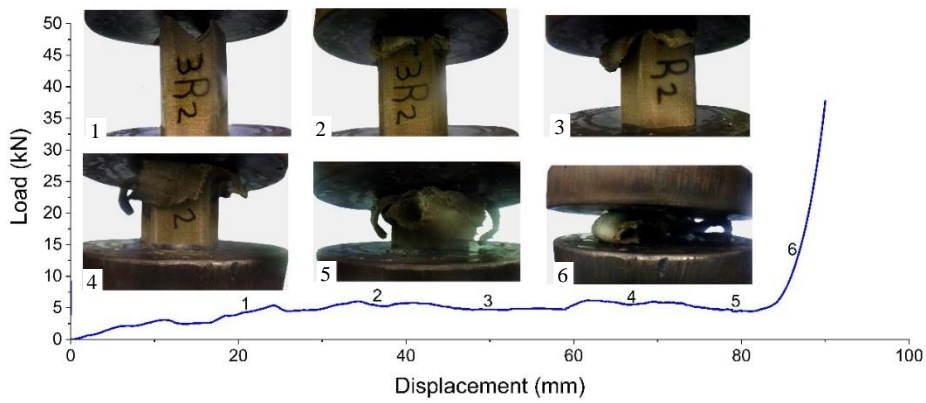


Fig.6. Representative Load vs displacement and collapse history of Corrugated with 2 layers specimen

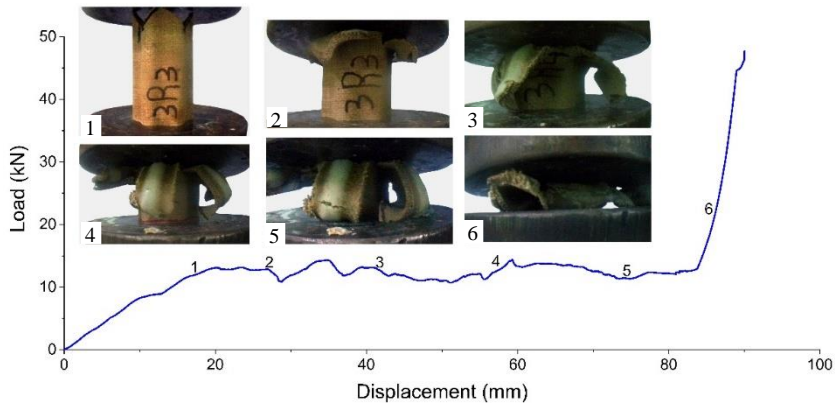


Fig.7. Representative Load vs displacement and collapse history of Corrugated with 3 layers specimen

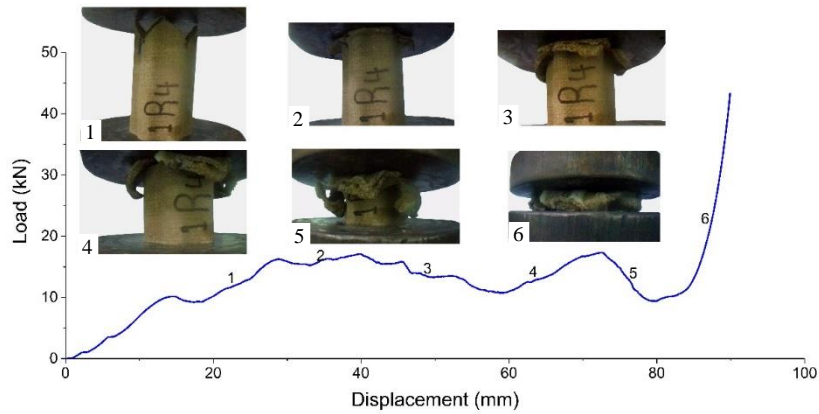


Fig.8. Representative Load vs displacement and collapse history of Corrugated with 4 layers specimen

3.2 INFLUENCE OF VARIOUS FACTORS ON CRASHWORTHINESS PARAMETERS OF JFRP SPECIMENS

Depending on the results, it is obvious that the effect of layers number, geometrical shape, and temperature treatment on crashworthiness parameters. In this section have been discussed and compared the obtained results to determine the appropriate energy-absorption design

3.2.1 Effect of plies laminate number

From the current results, it is very clear that there is a correlation between the plies laminate number and crashworthiness parameters for JFRP specimens are illustrated in Fig.9. Obviously that in terms of energy absorption (EA), peak load (P_{max}), and the mean load (P_m), these values rise up considerably with a further in the laminate number from 2 to 4 plies, which are independent of the geometrical shape of the specimens. These increases of values in the EA, P_{max} , and P_m are quite apparent for the specimen with 4-ply laminate, i.e. the EA and P_{max} of corrugated and circular cross-section profile are 17.310 kN and 964.079 J and 14.063 kN and 720.251 J, respectively. For all the specimens, the increase in EA and P_{max} is directly attributed to the increase in wall thickness of the specimen. The data indicate that the absorbed energy capability of the JFRP structure is strongly depends on the wall thickness (number of laminate plies). A specimen with a large thickness is able to absorb more energy, which in turn increases energy dissipation along its length. Yan and Chow [42] and Oshkovr et al. [43], found a similar phenomenon in their previous study. With respect to specific energy-absorption (SE) and crushing efficiency (η_c) of both types of specimens, these values increment noticeably for a specimen with laminate plies from 2 to 3. i.e. the SE and η_c values for Circular and corrugated cross-section formation with two and three layers are 24.26 J/g and 71.3%, and 30.92 J/g and 77.8% respectively as reported by Yan et al. [4] and Liu et al.[44]. On another hand, it is obvious that independent from 3 to 4 plies, the decrease in SE and η_c value, i.e. the SE of the corrugated specimen with 4 layers is less than the same specimen with 3 layers by 30.3%, and η_c by 10.5% respectively. In summary, the impact of specimen wall thickness to specimen diameter (t/D) ratio on load and absorb energy can be concluded based on the obtained test results. In the case of the same geometrical shape, the t/D ratio increases when the specimen wall layers increase from 2 to 4- laminate

plies. The correlation between t/D ratio and crashworthiness parameters of jute mat/epoxy structure is as noted: a growing in t/D ratio leads to an increase in TEA, P_{max} , and P_m . The grow in energy absorption ability, peak force, and the mean force is attributed to an increase in t/D ratio for jute mat/epoxy specimen, as depicted in Fig.9. That's mean, at a specific structure shape, a jute mat/epoxy specimen with larger numbers of laminate plies (larger wall thickness) exhibits higher resistance in deformation with higher values of energy dissipate, mean load and maximum peak load during axial deformation test.

3.2.2 Effect of geometrical shape

The influence of specimen cross-section shape on the crashworthiness parameters can be obviously noticed from Fig.9. The magnitudes of EA, P_{max} , and P_m of all the specimens with corrugated cross-section shapes are higher value than the specimens with circular cross-section shapes, when the number of plies is equal. For the P_{max} , combining the examined peak loads of jute mat/epoxy tubes with different laminate layers (2, 3 and 4 laminate plies) presented in the current work. From the obtained results, it can be said that there is a clear relationship between the geometrical shape and the peak load during the axial loading test. Indeed, the values of the peak loads are highly determined by the combined influence of plies laminate (wall thickness) and the cross-section shape of the tube. Mathew et al. [11] also state this trend in the previous study. The tube with the corrugated section exhibited the larger peak load (P_{max}) with a value of 17.31 kN than circular section specimen for the 4- laminates plies (Fig.9b). This result is also in line with the reported of the previous study by Eshkoo et al. [45].

For the EA, the influence of the geometrical shape on EA is depicted in Fig.9a. It is evidenced that EA values are dependent on the cross-section shape, in addition, the layers number of the tested specimens. The tubes with corrugated shape exhibited the maximum energy absorption, with a value of 964.079 for the 4-layers tube under the axial crushing loading effect. However, the use of (SE) is a mean parameter when valuation the Energy absorption abilities of structures made of different materials. In General, the higher the values of the SE, the more effective the energy absorber. Corrugated cross-section specimen exhibited a larger (SE) value of (30.918 J/g with 3 layers) than circular composite specimens series as exhibited in Fig.9d. The reason was that a specimen with a corrugated pattern has a longer

deformation/displacement up to the end of crushing, which depends on the cross-section geometry (specific laminate layers and sectional shape) of the component. Therefore, this proves that the geometrical shapes have the most important influence on the crashworthiness performance of jute mat/epoxy structures. This phenomenon agrees with the previous report by Palanivelu et al. [46] and Alkbir et al. [47].

For the mean crushing load (P_m), the examine observations might be attributed to the nature of the failure mechanisms for each one of different specimen geometry types in the post-deformation phase, which based on the cross-section geometry (tube shape) independent of the number of the layers, which agrees with the stated by Meran [48]. The load/displacement diagram of jute mat/epoxy specimens under uniaxial collapsing based on the manner of crush. For jute mat/epoxy specimens that are undergone to axial collapsing, the failure behaviour of the specimens appears to influence the loading stability. Compared with specimens with a circular pattern, the specimens with a corrugated pattern may

crush in a controlled manner and more stable with less sharp fluctuations in the value of load under the collapsing. This points out that the geometrical shape has a critical effect on the crashworthiness performance of composite structures.

For crush efficiency (η_c), the mean load (P_m) plays a significant role in representing the crashworthiness performance because of crush load efficiency. The more mean load (P_m) approaches to peak load, lead to a diminishing in acceleration and thus the efficiency is as highest as possible. It is essential to be the (η_c) close to 1 for great energy absorbing. The deviation in the value of efficiency points out a fast change in acceleration. Fig.9e. gives the influence of geometrical shape on the average η_c of the tubes. The corrugated pattern with 3 layers has the highest η_c value of 77.8%. This data proves that a cross-section pattern with a specific number of laminate plies may occur for jute

mat/epoxy specimens to attain η_c value with less scatters, which agrees with the previous study by Liu et al. [49].

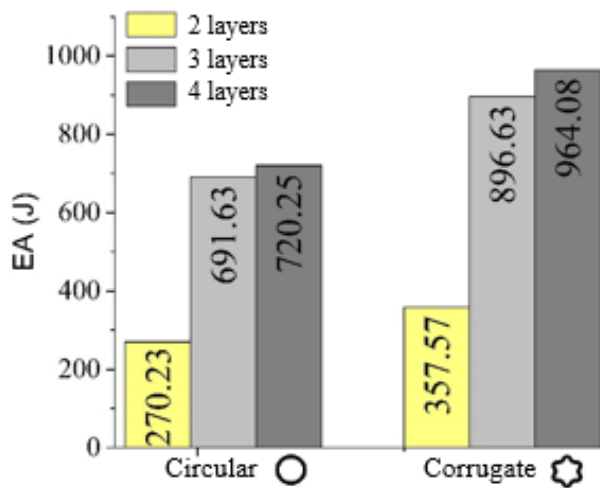


Fig.9a. Comparison EA (J) for composite circular and corrugated specimens at different laminate layers

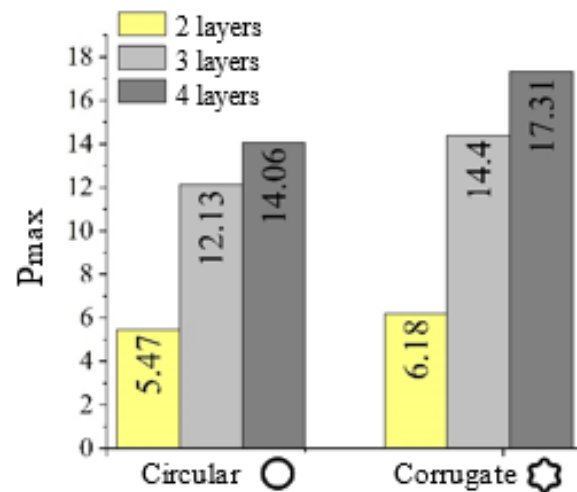


Fig.9b. Comparison P_{max} (kN) for composite circular and corrugated specimens at different laminate layers

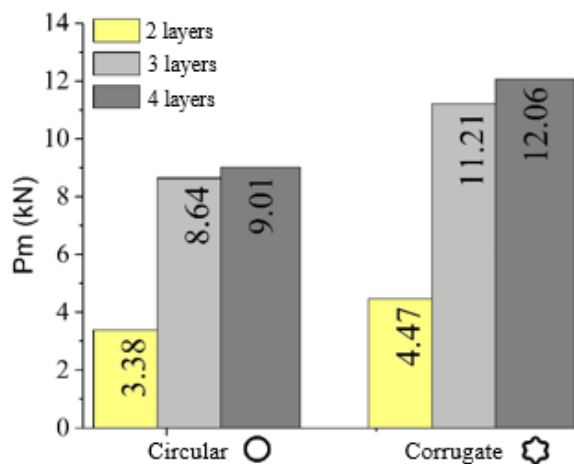


Fig.9c. Comparison P_m (kN) for composite circular and corrugated specimens at different laminate layers

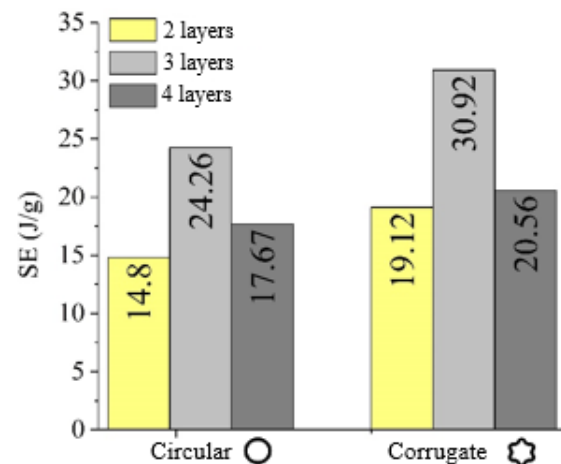


Fig.9d. Comparison SE (J/g) for composite circular and corrugated specimens at different laminate layers

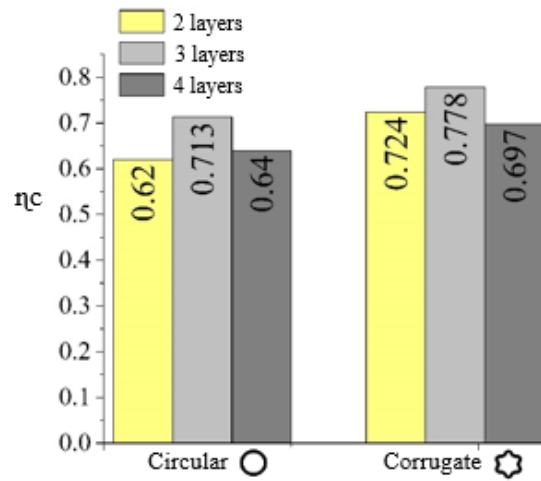


Fig.9e. Comparison η_c (%) for composite circular and corrugated specimens at different laminate layers

3.2.3 EFFECT OF TEMPERATURE TREATMENT

The crashworthiness parameters including P_{max} is depicted in fig.9b. The initial peak load must be as low as possible value and within the permissible limits of energy to avoid increased acceleration, which is closely related with permanent deformation and injuries to passengers in the car's cabin [50]. However, in addition to the effect of the trigger to reduce peak load on composite structures, in this experiment, the effective effect of temperature treatment on the peak load and crushing efficiency would be demonstrated. In order to prove that, it is necessary to compare current work with patterns holding the same used material, design, and technique in preparing the structure, in addition to the test conditions. Fig. 10 shows the variation of peak load values for the jute mat/epoxy composite specimens with three laminate plies, 100 mm in length, tulip trigger, under the same quasi-static test conditions, but without or with graded temperature treatment (i.e. at ambient temperature ($25 \pm 2 \text{ C}^0$) for 24h, 60 C^0 for 8h, and 100 C^0 for

4 h). It is obvious can notice that there is a decrease in P_{max} of circular JFRP specimens with temperature treatment (TT) by 55.5 % and 62.8 % respectively as compared to circular at 27.23 kN value Sivagurunathan et al. [51], and square at 32.58 kN Sivagurunathan et al. [32] of JFRP specimens without temperature treatment (No TT) as shown in fig.10a. This decrement was 47.1 % and 55.8 % respectively for corrugated JFRP specimen in current work as shown in Fig.10b. This clearly indicated to increase in the expansion of reinforcement and epoxy due to temperature treatment, the variance in the expansion led to generate the void and micro-cracks in the matrix and at the interface of specimens as shown Fig.11. On applying the load, it led to the propagation of the micro-crack into a major crack due to a decrease in the flexural strength, thus, it will a reduction in the load. This conclusion in line with previous studies by Xu et al. [12], and Shukla [52].

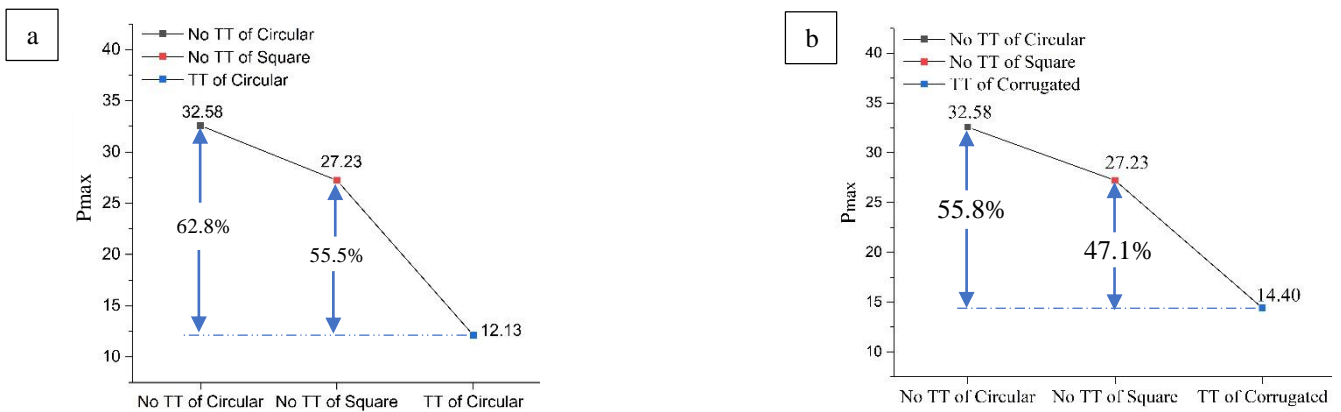


Fig.10. Variation of P_{max} for with and without temperature treatment for (a) Circular specimen and (b) Corrugated specimen.

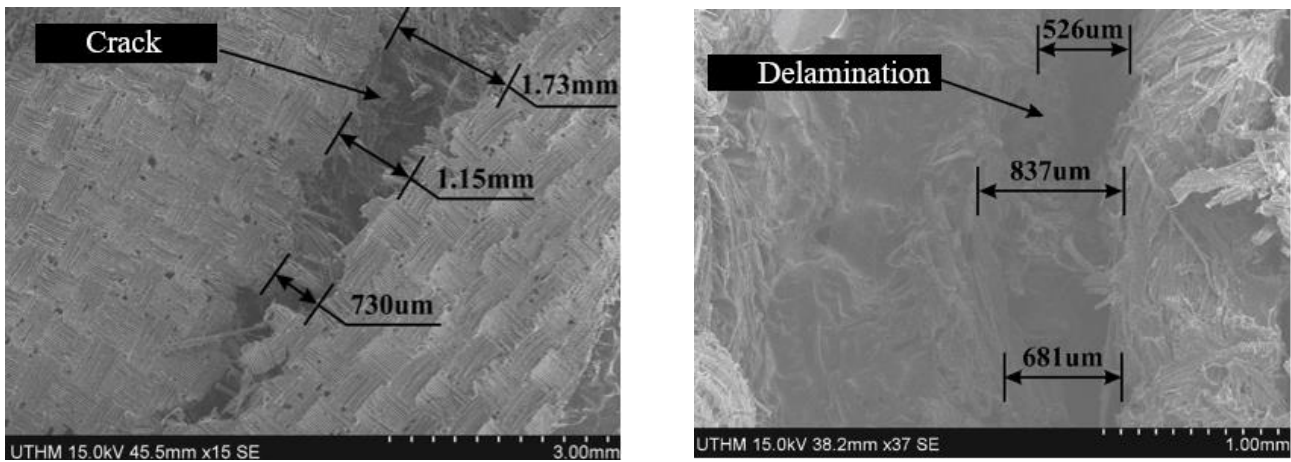


Fig.11. Representative the propagation of the micro-crack (left side) and delamination (right side) for reinforcement and epoxy.

4. COMPARISON

In order to evaluate the current work, a comparison must be made with previous studies. SE was chosen to provide a means for a fair comparison, due to it is considered the primary criterion for providing the highest levels of safety in the passenger compartment during a collision. From table 2, we can clearly see that corrugated JFRP structure with 3 layers achieved highly competitive results compared to other studies.

Thus, there is considerable potential to be a superior alternative to structures made of (minerals, synthetic fibers such as carbon and glass, and natural fibers).

Apart from that, using appropriate NFRP can have a higher mean load. This means there are still have room for the NFRP to be studied for improvisation.

Table II
Comparison of the current study with previous researches

Material	Geometrical Shape	Dimension, mm	Thickness, mm, (layers)	Crush effect	SEA, J/g	Ref.
Jute/epoxy	Corrugate circle	50×100	2 ,3, 4 L	Geometry	30.92 24.26	Current study
aluminium	square	50×50×180	1 – 3.25 mm	graded thickness	5.52 - 14.21	(Sun 2017),[53]
aluminium	square	50×50×250	2 mm	V-notch and groove initiators	6.09 - 8.27	(Balaji and Annamalai 2017), [54]
Glass/epoxy with four types of fillers used Rice husk, Wood Chips, Aluminum chips, and Coconut fibres.	Corrugated circle	100×100	2.5 mm	different geometries and with different types of fillers	16.3 – 20.7 11.7 – 18.98	(Al-Qrimli et al. 2015), [55].
E-glass/epoxy Carbon/epoxy	circle	44×150	3 L	Fibres orientation	4.194 – 7.200 6.100 – 10.283	(Mohamed and Kumar 2017), [56].
Glass/epoxy	square cylindrical hexagonal decagonal	36 ×120	1.829 mm	different types of triggers on crashworthiness for different types of geometries	3.79 – 4.38 4.00 – 4.24 4.27 – 4.93 5.97 – 7.35	(Hussain, Regalla, and Rao Yendluri 2017), [57].
glass/epoxy	Circle corrugated	160 ×150	6 L	Effect of geometry	10.2 12.2	(Abdewi et al. 2006), [5].
Carbon/epoxy	cylindrical	44×150	3 mm	Effect of orientation	6.10- 10.28	M.Nalla et al.(2017),[58].
Ramie/epoxy	square	80×80×50	12 L 24 L 30 L	effect of layers	5.5 12.4 16.5	(Ghoushji et al. 2016), [59].
Kenaf/epoxy	square	40×40× 350	5 mm	unidirectional and random orientation	22.4	(Said, Lau, and Yaakobc 2017), [60].
silk/epoxy	square	80×80 ×50 80 ×80 ×80 80 ×80 ×120	12 ,24 ,30 L 12, 24, 30 L 12 ,24, 30 L	effect of trigger on crashworthiness for different length and layers	5 - 16 4.2 – 11.6 3.8 - 14	(Eshkoor et al. 2015), [45].

CONCLUSION

in this work has been investigated the effect of geometrical shape, a number of laminate layers as well as temperature treatment and their combined influence on crashworthiness characteristic and capability of energy absorption of jute mat/epoxy composite tubes. Consideration was given to adopting two types of geometric shapes, which are (corrugated and circular), with three different thicknesses (two, three and four layers), both of which were treated thermally. For each specimen was tested under quasi-static loading. The purpose of this work is to design and manufacture an appropriate energy absorption device by employing natural fibres reinforcement. The work reveals the conclusion as the following:

- I. Both types of specimens exhibited a stable and progressive crushing manner rather than catastrophic deformation, the potential to be an energy-absorbing device.
- II. The geometric shape had demonstrated to have a big influence on SEA and η_c , where the corrugated JFRP tubes with three layers exhibited a higher value for SEA and η_c compared to the circular composite tubes.
- III. With the growth in a number of laminated plies, the P_{max} , P_m and the TEA increased. Specimens with a large number of laminate layers dissipated more energy along their length and show higher resistance of the load.
- IV. In addition to the effect of a trigger, the temperature treatment of the JFRP patterns exhibited that they contribute significantly to reducing peak load, but increase crushing efficiency remarkably. Comparing with the previous studies that have the same material, design, and technique in fabricating but without temperature treatment, e.g. For circular JFRP specimen with three laminate layers, The peak load of temperature-treated patterns decreased from 32.58 kN to 12.13 kN, but the crushing efficiency increased from 67% to 71.3% compared to patterns with no temperature-treated.

The optimal design of jute/epoxy structures, in the tubes selected for corrugated shape in the current study, has a SE of 30.918 J/g and η_c of 77.8%. Which outperforms to energy absorption in many previous studies which including (conventional metal, synthetic composite, and Natural composite) structures that mentioned in literature.

Acknowledgement

The authors wish to thank University Technical Malaysia Melaka for the support for this research.

REFERENCES

- [1] M. F. M. Alkbir, S. M. Sapuan, A. A. Nuraini, and M. R. Ishak, "Effect of geometry on crashworthiness parameters of natural kenaf fibre reinforced composite hexagonal tubes," *Mater. Des.*, vol. 60, no. 1, pp. 85–93, 2014.
- [2] A. E. Ismail, "Kenaf Fiber Reinforced Composites Tubes as Energy Absorbing Structures," no. 01, pp. 2–6, 2016.
- [3] A. G. Mamalis, D. E. Manolacos, M. B. Ioannidis, and D. P. Papapostolou, "On the crushing response of composite sandwich panels subjected to edgewise compression: Experimental," *Compos. Struct.*, vol. 71, no. 2, pp. 246–257, 2005.
- [4] L. Yan, N. Chouw, and K. Jayaraman, "Effect of triggering and polyurethane foam-filler on axial crushing of natural flax/epoxy composite tubes," *Mater. Des.*, vol. 56, pp. 528–541, 2014.
- [5] E. F. Abdewi, S. Sulaiman, A. M. S. Hamouda, and E. Mahdi, "Effect of geometry on the crushing behaviour of laminated corrugated composite tubes," *J. Mater. Process. Technol.*, vol. 172, no. 3, pp. 394–399, 2006.
- [6] S. Xie, W. Yang, N. Wang, and H. Li, "Crashworthiness analysis of multi-cell square tubes under axial loads," *Int. J. Mech. Sci.*, vol. 121, no. November 2016, pp. 106–118, 2017.
- [7] H. El-hage, P. K. Mallick, and N. Zamani, "A numerical study on the quasi-static axial crush characteristics of square aluminum – composite hybrid tubes," vol. 73, pp. 505–514, 2006.
- [8] E. Mahdi, A. M. S. Hamouda, and T. A. Sebaey, "The effect of fiber orientation on the energy absorption capability of axially crushed composite tubes," *Mater. Des.*, vol. 56, pp. 923–928, 2014.
- [9] M. Iqbal, M. Islam, J. Ananda, and K. Lau, "Potentiality of utilising natural textile materials for engineering composites applications," *J. Mater.*, vol. 59, pp. 359–368, 2014.
- [10] S. Ochelski and P. Gotowicki, "Experimental assessment of energy absorption capability of carbon-epoxy and glass-epoxy composites," *Compos. Struct.*, vol. 87, no. 3, pp. 215–224, 2009.
- [11] A. T. Mathew and A. Thakur, "Experimental study on crushing performance of different geometrical structures woven natural silk epoxy composite tubes," vol. 8, no. 8, pp. 55–66, 2017.
- [12] J. Xu, Y. Ma, Q. Zhang, T. Sugahara, Y. Yang, and H. Hamada, "Crashworthiness of carbon fiber hybrid composite tubes molded by filament winding," *Compos. Struct.*, vol. 139, pp. 130–140, 2016.
- [13] X. Nguyen, S. Hou, T. Liu, and X. Han, "A potential natural energy absorption material - Coconut Mesocarp: Part A: Experimental Investigations on Mechanical Properties," *Int. J. Mech. Sci.*, 2016.
- [14] M. F. M. Alkbir, S. M. Sapuan, A. A. Nuraini, and M. R. Ishak, "The Effect of Fiber Content on the Crashworthiness Parameters of Natural Kenaf Fiber-Reinforced Hexagonal Composite Tubes," vol. 11, no. 1, pp. 75–86, 2016.
- [15] J. Huang and X. Wang, "Effect of the SMA Trigger on the Energy Absorption Characteristics of CFRP Circular Tubes," 2010.
- [16] L. N. S. Chiu *et al.*, "Crush responses of composite cylinder under quasi-static and dynamic loading," *Compos. Struct.*, vol. 131, pp. 90–98, 2015.
- [17] A. U. Ude, R. A. Eshkooor, and C. H. Azhari, "Crashworthy Characteristics of Axial Quasi-statically Compressed Bombyx mori Composite Cylindrical Tubes : Experimental," vol. 18, no. 8, pp. 1594–1595, 2017.
- [18] C. Parameters, H. S. S. Aljibori, K. Firas, M. Alosfur, and N. J. Ridha, "Axial quasi-static crushing behaviour of cylindrical woven kenaf fiber reinforced composites Axial quasi-static crushing behaviour of cylindrical woven kenaf fiber reinforced composites," 2017.
- [19] S. Palanivelu *et al.*, "Crushing and energy absorption performance of different geometrical shapes of small-scale glass / polyester composite tubes under quasi-static loading conditions," *Compos. Struct.*, vol. 93, no. 2, pp. 992–1007, 2011.
- [20] E. F. Abdewi, S. Sulaiman, A. M. S. Hamouda, and E. Mahdi, "Quasi-static axial and lateral crushing of radial corrugated composite tubes," *Thin-Walled Struct.*, vol. 46, no. 3, pp. 320–332, 2008.
- [21] C. T. F. Ross, B. Hock, T. Boon, M. Chong, and M. D. A. Mackney, "The buckling of GRP hemi-ellipsoidal dome shells under external hydrostatic pressure," vol. 30, pp. 691–705, 2003.
- [22] C. McGregor, R. Vaziri, A. Poursartip, and X. Xiao, "Axial crushing of triaxially braided composite tubes at quasi-static and dynamic rates," *Compos. Struct.*, vol. 157, pp. 197–206, 2016.
- [23] A. Rabiee and H. Ghasemnejad, "Progressive Crushing of Polymer Matrix Composite Tubular Structures : Review," pp. 14–48, 2017.
- [24] M. B. Azimi and M. Asgari, "Energy absorption characteristics and a meta-model of miniature frusta under axial impact," vol. 11, no. 1, pp. 75–86, 2016.
- [25] B. Rezaei, A. Niknejad, H. Assaei, and G. H. Liaghat, "Axial splitting of empty and foam-filled circular composite tubes - An experimental study," *Arch. Civ. Mech. Eng.*, vol. 15, no. 3, pp. 650–662, 2015.
- [26] J. Xu, Y. Ma, Q. Zhang, T. Sugahara, Y. Yang, and H. Hamada, "Crashworthiness of carbon fiber hybrid composite tubes molded by filament winding," *Compos. Struct.*, vol. 139, pp. 130–140, 2016.
- [27] Y. Ma, T. Sugahara, Y. Yang, and H. Hamada, "A study on the energy absorption properties of carbon / aramid fiber filament winding composite tube," *Compos. Struct.*, vol. 123, pp. 301–311,

- 2015.
- [28] G. L. Farley, "Energy Absorption of Composite Materials," *J. Compos. Mater.*, vol. 17, no. 3, pp. 267–279, 1983.
- [29] G. L. Farley, "Effect of specimen geometry on the energy absorption of composite materials," *J. Compos. Mater.*, vol. 20, no. July, p. 390, 1986.
- [30] D. D. Melo, L. S. Silva, and J. E. N. Villena, "The effect of processing conditions on the energy absorption capability of composite tubes," vol. 82, pp. 622–628, 2008.
- [31] H. Jiang, Y. Ren, B. Gao, J. Xiang, and F. Yuan, "International Journal of Mechanical Sciences Design of novel plug-type triggers for composite square tubes : enhancement of energy-absorption capacity and inducing failure mechanisms," vol. 132, no. June, pp. 113–136, 2017.
- [32] R. Sivagurunathan, S. Lau, T. Way, L. Sivagurunathan, and M. Y. Yaakob, "Effects of triggering mechanisms on the crashworthiness characteristics of square woven jute / epoxy composite tubes," 2018.
- [33] A. Kumar and A. Srivastava, "Industrial Engineering & Management Preparation and Mechanical Properties of Jute Fiber Reinforced Epoxy Composites," vol. 6, no. 4, pp. 4–7, 201
- [34] D. Y. Hu, M. Luo, and J. L. Yang, "Experimental study on crushing characteristics of brittle fibre/epoxy hybrid composite tubes," *Int. J. Crashworthiness*, vol. 15, no. 4, pp. 401–412, 2010.
- [35] E. Mahdi and T. A. Sebaey, "An experimental investigation into crushing behavior of radially stiffened GFRP composite tubes," *Thin-Walled Struct.*, vol. 76, pp. 8–13, 2014.
- [36] H. Hadavinia and H. Ghasemnejad, "Effects of Mode-I and Mode-II interlaminar fracture toughness on the energy absorption of CFRP twill / weave composite box sections," *Compos. Struct.*, vol. 89, no. 2, pp. 303–314, 2009.
- [37] M. N. Roslan, M. Y. Yahya, Z. Ahmad, and A. R. A. Hani, "Energy absorption behaviour of braided basalt composite tube," *Adv. Compos. Mater.*, no. November, pp. 1–15, 2017.
- [38] G. Belingardi, "ScienceDirect ScienceDirect Axial crushing of metal-composite hybrid tubes : experimental Axial crushing tubes : experimental analysis hybrid analysis Thermo-mechanical a high Simonetta Boria modeling airplane gas turbine," *Procedia Struct. Integr.*, vol. 8, pp. 102–117, 2018.
- [39] A. Eyvazian, M. K. Habibi, A. Magid, and R. Hedayati, "Axial crushing behavior and energy absorption efficiency of corrugated tubes," *Mater. Des.*, vol. 54, pp. 1028–1038, 2014.
- [40] S. T. W. Lau, M. R. Said, and M. Y. Yaakob, "On the effect of geometrical designs and failure modes in composite axial crushing: A literature review," *Compos. Struct.*, vol. 94, no. 3, pp. 803–812, 2012.
- [41] Palanivelu S et al., "Comparative study of the quasi-static energy absorption of small-scale composite tubes with different geometrical shapes for use in sacrificial cladding structures," *Compos. Struct.*, no. 0, pp. 1–22, 2011.
- [42] L. Yan and N. Chouw, "Crashworthiness characteristics of flax fibre reinforced epoxy tubes for energy absorption application," *Mater. Des.*, vol. 51, pp. 629–640, 2013.
- [43] S. A. Oshkovr, R. A. Eshkoo, S. T. Taher, A. K. Ariffin, and C. H. Azhari, "Crashworthiness characteristics investigation of silk/epoxy composite square tubes," *Compos. Struct.*, vol. 94, no. 8, pp. 2337–2342, 2012.
- [44] Q. Liu, H. Xing, Y. Ju, Z. Ou, and Q. Li, "Quasi-static axial crushing and transverse bending of double hat shaped CFRP tubes," *Compos. Struct.*, vol. 117, pp. 1–11, 2014.
- [45] R. A. Eshkoo, A. U. Ude, A. B. Sulong, R. Zulki, A. K. Arif, and C. H. Azhari, "Energy absorption and load carrying capability of woven natural silk epoxy e triggered composite tubes," vol. 77, pp. 10–18, 2015.
- [46] S. Palanivelu et al., "Composites : Part B Comparison of the crushing performance of hollow and foam-filled small-scale composite tubes with different geometrical shapes for use in sacrificial cladding structures," *Compos. Part B*, vol. 41, no. 6, pp. 434–445, 2010.
- [47] M. F. M. Alkbir, S. M. Sapuan, A. A. Nuraini, and M. R. Ishak, "Fiber properties and crashworthiness parameters of natural fiber-reinforced composite structure: A literature review," *Compos. Struct.*, 2016.
- [48] A. P. Meran, "Solidity effect on crashworthiness characteristics of thin-walled tubes having various cross-sectional shapes," vol. 8265, no. December, 2015.
- [49] Q. Liu, Z. Ou, Z. Mo, Q. Li, and D. Qu, "Experimental investigation into dynamic axial impact responses of double hat shaped CFRP tubes," *Compos. Part B Eng.*, vol. 79, pp. 494–504, 2015.
- [50] R. A. Eshkoo, S. A. Oshkovr, A. B. Sulong, R. Zulkipli, A. K. Ariffin, and C. H. Azhari, "Effect of trigger configuration on the crashworthiness characteristics of natural silk epoxy composite tubes Composites : Part B," *Compos. Part B*, vol. 55, no. December, pp. 5–10, 2013.
- [51] R. Sivagurunathan, S. Lau, and T. Way, "The Effects of Triggering Mechanisms on the Energy Absorption Capability of Circular Jute / Epoxy Composite Tubes under Quasi-Static Axial Loading," 2018.
- [52] M. J. Shukla, "Elevated temperature performance of hybrid polymer composites Elevated temperature performance of hybrid polymer composites," 2015.
- [53] G. Sun, "Thin-Walled Structures Energy absorption mechanics for variable thickness thin-walled structures," *Thin Walled Struct.*, vol. 118, no. April, pp. 214–228, 2017.
- [54] G. Balaji and K. Annamalai, "An experimental and numerical scrutiny of crashworthiness variables for square column with V-notch and groove initiators under quasi-static loading," *Cogent Eng.*, vol. 21, no. May, pp. 1–20, 2017.
- [55] H. F. Al-Qrimli, F. A. Mahdi, F. B. Ismail, and I. S. Alzorqi, "Thin-walled composite tubes using fillers subjected to quasistatic axial compression," *IOP Conf. Ser. Mater. Sci. Eng.*, vol. 78, no. 1, 2015.
- [56] M. N. Mohamed and A. P. Kumar, "Numerical and Experimental Study of the Effect of Orientation and Stacking Sequence on Petalling of Composite Cylindrical Tubes under Axial Compression," *Procedia Eng.*, vol. 173, pp. 1407–1414, 2017.
- [57] N. N. Hussain, S. P. Regalla, and V. D. Rao Yendluri, "Numerical investigation into the effect of various trigger configurations on crashworthiness of GFRP crash boxes made of different types of cross sections," *Int. J. Crashworthiness*, vol. 22, no. 5, pp. 565–581, 2017.
- [58] K. M. Nalla Mohamed, "Numerical and experimental study of the effect of orientation and stacking sequence on petalling of composite cylindrical tubes under axial compression," *ScienceDirect*, vol. 173, pp. 1407–1414, 2017.
- [59] M. J. Ghoushji, S. Abdullah, R. Zulkipli, A. B. Sulong, and C. H. Azhari, "EFFECT OF LAYER STACKING NUMBER ON CRASHWORTHINESS CHARACTERISTICS OF WOVEN NATURAL RAMIE EPOXY," no. February, pp. 17–18, 2016.
- [60] M. R. Said, S. T. W. Lau, and M. Y. Yaakob, "Quasi static axial crushing of kenaf fibre reinforced epoxy composite fabricated by VARTM method," *ARPJ J. Eng. Appl. Sci.*, vol. 12, no. 16, pp. 4804–4808, 2017.